

USP39-mediated deubiquitination of Cyclin B1 promotes tumor cell proliferation and glioma progression

Yue Xiao^a, Xinyi Chen^a, Weiwei Hu^b, Wenjing Ma^a, Qianqian Di^a, Haimei Tang^a, Xibao Zhao^a, Guodong Huang^a, Weilin Chen^{a,c,*}

^a Guangdong Provincial Key Laboratory of Regional Immunity and Diseases, Department of Neurosurgery, Shenzhen Second People's Hospital, The first Affiliated Hospital of Shenzhen University, Shenzhen University Medical School, Shenzhen 518055, China

^b Department of Neurosurgery, Second Affiliated Hospital, Zhejiang University School of Medicine, Hangzhou 310058, China

^c Institute of Biological Therapy, Shenzhen University, Shenzhen 518055, China

ARTICLE INFO

Keywords:

Cyclin B1
Cell cycle
Deubiquitinase
Glioma
USP39

ABSTRACT

Background: The elevated Cyclin B1 expression contributes to various tumorigenesis and poor prognosis. Cyclin B1 expression could be regulated by ubiquitination and deubiquitination. However, the mechanism of how Cyclin B1 is deubiquitinated and its roles in human glioma remain unclear.

Methods: Co-immunoprecipitation and other assays were performed to detect the interacting of Cyclin B1 and USP39. A series of *in vitro* and *in vivo* experiments were performed to investigate the effect of USP39 on the tumorigenicity of tumor cells.

Results: USP39 interacts with Cyclin B1 and stabilizes its expression by deubiquitinating Cyclin B1. Notably, USP39 cleaves the K29-linked polyubiquitin chain on Cyclin B1 at Lys242. Additionally, overexpression of Cyclin B1 rescues the arrested cell cycle at G2/M transition and the suppressed proliferation of glioma cells caused by USP39 knockdown *in vitro*. Furthermore, USP39 promotes the growth of glioma xenograft in subcutaneous and *in situ* of nude mice. Finally, in human tumor specimens, the expression levels of USP39 and Cyclin B1 are positively relevant.

Conclusion: Our data support the evidence that USP39 acts a novel deubiquitinating enzyme of Cyclin B1 and promoted tumor cell proliferation at least in part through Cyclin B1 stabilization, represents a promising therapeutic strategy for tumor patients.

Introduction

Cyclin B1 (*CCNB1*) is an important member of cyclin protein family, a group of cell cycle regulatory molecules. During cell cycle progression, the accumulation of Cyclin B1 begins at S phase and reaches the highest level at G2/M transition, and then the protein is rapidly degraded at metaphase-anaphase transition [1]. Synthesis of Cyclin B1 leads to the formation of the complex with Cyclin-dependent kinase 1 (CDK1). The Cyclin B1/CDK1 heterodimer promotes cell cycle transition from G2 to M phase and maintains the orderly progression of cell cycle [2]. However, overexpression of Cyclin B1 may lead to uncontrolled cell proliferation. Furthermore, abnormal expression of Cyclin B1 has been reported in several different human cancers [3–6]. In most of these reports the high expression level of Cyclin B1 was associated with a poor

clinical outcome of patients. Therefore, it is important to explore the molecular mechanism on the regulation of Cyclin B1 expression in the pathogenesis and development of human cancer.

Regulation of Cyclin B1 expression is complicated and often occurs at the transcriptional and post-transcriptional, as well as post-translational levels. The transcription of Cyclin B1 could be promoted by CREPT (cell cycle-related and expression-elevated protein in tumor) /Aurora B complex to accelerate the G2/M transition in gastric cancer [6]. RNA-binding motif protein 43 (RBM43) directly associated with the 3'UTR of Cyclin B1 mRNA and negatively regulated its expression, resulting in the inhibition of tumor growth and liver carcinogenesis [7]. Besides, activation of E3 ligase APC/C (anaphase promoting complex or cyclosome)-CDC20 mediates the degradation of Cyclin B1 by the proteasomal pathway, facilitating anaphase onset [8,9]. Furthermore, it

Abbreviations: USP, Ubiquitin Specific Peptidase; TMA, Tissue microarrays; IHC, Immunohistochemistry; CHX, Cycloheximide; H&E, Hematoxylin-eosin.

* Corresponding author at: 1066 Xueyuan Avenue, Shenzhen 518055, China.

E-mail address: cwl@szu.edu.cn (W. Chen).

<https://doi.org/10.1016/j.tranon.2023.101713>

Received 15 March 2023; Received in revised form 4 June 2023; Accepted 7 June 2023

Available online 9 June 2023

1936-5233/© 2023 The Authors. Published by Elsevier Inc. This is an open access article under the CC BY-NC-ND license (<http://creativecommons.org/licenses/by-nc-nd/4.0/>).

was found that USP14 promoted G2/M cell cycle transition of breast cancer cells by deubiquitinating and upregulating Cyclin B1 [10]. However, whether other USPs upregulate Cyclin B1 expression in human glioma remain unknown.

Here, we demonstrate that crosstalk between the two oncogenes, *USP39* and *CCNB1*, has an important role in the development of human glioma. USP39 is a deubiquitinating enzyme containing the ubiquitin specific protease domain and the UBP (ubiquitin-specific processing protease) -type zinc finger domain [11]. We found that USP39 could upregulate Cyclin B1 protein stability to promote G2/M cell cycle transition and glioma cell proliferation, as well as tumor growth *in vivo*. This study suggests that USP39-Cyclin B1 may represent a potential target in the treatment of glioma.

Materials and methods

Clinical specimens

The five human glioma tissues and tissue microarrays (TMA) containing 67 paraffin-embedded samples were from the department of Neurosurgery of the Second Affiliated Hospital, Zhejiang University, School of Medicine (Hangzhou, China). The detail information of specimens was described as our previous report [12]. 67 paraffin-embedded tissues samples were used for the analysis of the expression levels of USP39 and Cyclin B1 by immunohistochemistry. 6 frozen samples were subjected to the analysis of the expression levels of USP39 and Cyclin B1 in human glioma by Western blotting. The study was approved by the ethics committee of the Zhejiang University (Hangzhou, China) and Shenzhen University (Shenzhen, China) based on the ethical principles of the Helsinki Declaration. The patients provided their written informed consent to participate in this study.

Cell culture and transfection

U251, U87 and HEK293T cells were purchased from the Culture Collection of the Chinese Academy of Sciences (Shanghai, China). Cells are maintained in DMEM medium with 10%FBS and 1%PS. All the cell lines were kept at 37 °C under a humidified atmosphere of 5% CO₂ in an incubator, trypsinized, and passaged every 2–3 days. Plasmid DNA was transfected using JetPrime transfection reagents (Polyplus Transfection, New York, NY, USA).

Plasmids, antibodies and reagents

Flag-His-Cyclin B1 plasmid (#CH868243) was purchased from Vigene Biosciences (Shangdong, China). MYC-USP39, HA-USP39, HA-USP39-N, HA-USP39-C and V5-BTRC were constructed by standard molecular biology techniques by cloning into the pcDNA3.1 vector. HA-Ub and HA-K6-Ub, HA-K11-Ub, HA-K27-Ub, HA-K29-Ub, HA-K33-Ub, HA-K48-Ub, HA-K63-Ub plasmids were gifts from Prof. Xuetao Cao (National Key Laboratory of Medical Immunology, Shanghai, China). Individual ubiquitin constructs could only form ubiquitin linkages at a single lysine (for example, K48 indicates every lysine except K48 is changed to arginine). GST-USP39 plasmid was constructed by standard molecular biology techniques by cloning into the pGEX-4T-GST vector. The following antibodies were used: anti-Cyclin B1 (12231S, CST, Danvers, MA, USA), anti-USP39 (ab131244, Abcam, Cambridge, MA, USA), anti-Flag (A00187–100, GenScript, Piscataway, NJ, USA), anti-HA (51,064–2-AP, Proteintech, Wuhan, China), anti-MYC (A00704–100, GenScript), anti-Ubiquitin (3936, CST), anti-β-Actin (AA128, Hua An Biotechnology of China, Shangdong, China), anti-GAPDH (60,004–1-Ig, Proteintech). Reagents used in this study included the following: MG132 (#M8699), chloroquine (#C6628) and cycloheximide (#C4218) were purchased from Sigma-Aldrich, Merck, kGaA, Darmstadt, Germany. Puromycin Dihydrochloride (#ST551) was purchased from Beyotime Biotechnology, Shanghai, China.

RNA interference

2×10^5 U251 cells or U87 cells were plated in 12-well cell culture plates, incubated at 37 °C, 5%CO₂ incubator overnight. After the screening concentration of siRNA, 20 nM hUSP39-siRNA for U251 cells or U87 cells were added to 100 μl JetPrime buffer, adding 3 μl JetPrime transfection reagents and reacting at room temperature (RT) for 10 min, then added to transfection complexes into plates and following experiments were continued after 48 h or 72 h. The following sequence was targeted for human USP39 siRNA: 5'-GCAUAUGAUGGUACCACUUTT-3' 4 shRNAs (shRNA1: GATTTGGAAGAGCGGAGATAAT

CCAAGAGATTATCTCGCCTCTTCCAAATCTTTTTT, shRNA2: GTACTTCAAGGCCGGGG

TTTCAAGAGAACCCCGGCCTTGAAGTACTTTTTT, shRNA3: GTTGCTCCATATCTAAT

CTTTCAAGAGAAGATTAGATATGGAGGCAACTTTTTT, shRNA4: GCCTTCCAGACAAC

ATGAGATTTCAAGAGAATCTCATAGTTGTCTGGAAGGCTTTTTT) targeting USP39 (NM06590.4) were designed and inserted into lentivirus vector pLent-4 in 1 shRNA-GFP-Puro (Vigene. Inc. Shandong, China). Lentivirus was packaged in 293T cells and lentivirus titer was 1×10^8 /ml. 3 days after infection, U251 cells with stable knockdown USP39 were screened by GFP and puromycin. The knockdown efficiency of USP39 was determined by RT qPCR and Western blot.

Quantitative PCR

Total cellular RNA was isolated from cells using TRIzol reagent (Takara, Beijing, China) and subjected to quantitative PCR analysis for expression of mRNA. Data were determined by normalization of expression of β-actin in each sample. Analytik Jena qTOWER3 PCR system (Jena, Germany) was used for quantitative PCR. Gene-specific primer sequences were as following: hβ-ACTIN: 5'-CATGTACGTTGC-TATCCAGGC-3', 5'-CTCCTTAATGTACGCACGAT-3'; hUSP39: 5'-GGT TTGAAGTCTCACGCCTAC-3', 5'-GGCAGTAAACTTGAGGGTGT-3'; hCCNB1 exon 2–3: 5'-CAGGCCAAATGCCTATG –3', 5'-GTTCTGGC TCAGGTCT –3'; hCCNB1 intron 2: 5'-GTAACCTCTTCTCTGACC-3', 5'-GGCTGTAGATGAAACAGAG.

Immunoblot analysis and immunopurification

Cells were transfected expression plasmid for 24–30 h or transfected siRNA for 72 h. Cell lysed with $1 \times$ cell lysis buffer (CST) containing protease inhibitor mixture. For immunopurification, whole-cell extracts were collected 30 h after transfection and were lysed in immunoprecipitation buffer and containing protease inhibitor mixture. After centrifugation for 10 min at 12,000 g, supernatants were collected and incubated with Flag-M2 beads (Sigma-Aldrich) or protein A/G Plus-Agarose Immunoprecipitation reagent (Santa Cruz Biotechnology, Dallas, Texas, USA) together with 1 μg anti-HA or USP39 antibody. After overnight of incubation, beads were washed five times with immunoprecipitation buffer (0.5% Nonidet-P40, 100 mM NaCl, 1 mM EDTA and 20 mM Tris-Cl pH 8.0). Samples were boiled with 1% (wt/vol) SDS sample loading buffer. Equal amounts of protein were subjected to 10% SDS-PAGE and transferred onto nitrocellulose filter membranes (Millipore, Bedford, MA, USA). The membranes were blocked in 5% non-fat milk and immunoblotted overnight at 4 °C with primary antibodies, followed by their respective secondary antibodies.

Immunohistochemistry

Paraffin-embedded tumor tissues were cut into 5 μm paraffin sections, Sections for Immunohistochemical SABC staining were dewaxed in xylene, soaked with 100%, 95%, 90%, 80%, 70% ethanol and H₂O. Endogenous catalase activity was inactivated by H₂O₂. Sections were set in citrate buffer (PH6.0) and heated to fixed antigen. Then Sections were

put in a wet box and blocked by 5%BSA and incubated with 1:100 dilution of rabbit anti-USP39 antibody or anti-Cyclin B1 antibody at 4 °C overnight, and with the biotinylated goat anti-rabbit antibody with the streptavidin-peroxidase conjugate. Finally, the sections were developed using a 3,3'-diaminobenzidine (DAB) tetrahydrochloride substrate kit at room temperature for 1–5 min and then counterstained with hematoxylin. The percentage of positively stained cells and the staining intensity were calculated and analyzed by using image J software.

GST-pull down assay

Whole cell lysate containing Flag-Cyclin B1 protein was prepared in HEK293T cells. GST and GST-USP39 proteins were prepared in bacteria. GST fusion proteins were bound to Glutathione Sepharose 4B (#17,075,601, GE Healthcare, Milwaukee, WI, USA) for 3 h at 4 °C. Whole cell lysate containing Flag-Cyclin B1 protein was incubated with indicated GST fusion protein for 2 h at 4 °C. After washing with NETN buffer (0.5% Nonidet-P40, 100 mM NaCl, 1 mM EDTA and 20 mM Tris-Cl pH 8.0) for 5 times, the bound proteins were eluted and separated by SDS-PAGE and immunoblotting was performed with indicated antibodies.

In vitro deubiquitination assay

HEK293T cells were co-transfected with His-tagged Cyclin B1 and HA tagged K29-Ubiquitin for 24 h. After adding MG132 (20 μM) for 6 h, cells were lysed, and cell lysates were incubated with Ni-NAT agarose for 12 h at 4 °C. The incubated Ni-NAT agarose and protein complex were washed with washing buffer (50 mM Na₂HPO₄, 300 mM NaCl, 10 mM imidazole) for 5 times and the K29-Ub conjugate were eluted with elution buffer (50 mM Na₂HPO₄, 300 mM NaCl, 500 mM imidazole). *In vitro* deubiquitination assay was performed as described previously [13]. The K29-Ub conjugates and purified GST-USP39 or GST proteins were incubated with DUB buffer (50 mM HEPES (pH 7.5), 100 mM NaCl, 2 mM dithiothreitol, 1 mM MnCl₂ and 0.01% Brij-35) in a 37 °C water bath for 30 min, and the supernatants were collected after low-speed centrifugation, boiled with loading buffer, and analyzed by immunoblot. The specific detection of K29-Ub-CycB1 is performed by anti-HA immunoblot on GST-USP39 pulled material.

Protein stability assay

To assess Cyclin B1 protein turnover, cells were treated with cycloheximide (CHX) (0.1 mg/ml) and harvested at different time points. Harvested cells were then lysed in NETN buffer and the lysate samples were separated by SDS-PAGE and blotted with indicated antibodies. Finally, we quantified of the protein levels by ImageJ software (National Institute of Health, Bethesda, MD, USA).

Cell counting kit - 8 (CCK-8) assay

The proliferation of cells was measured using CCK-8 (Yeasen, Shanghai, China). Cells were seeded on the 6-well plate, U251 and U87 cells were treated with USP39-siRNA or scramble-siRNA for 48 h. Cells were digested, centrifuged, and diluted to 1 × 10⁵/ml with DMEM containing 10% FBS, and 100 μl cell suspensions were seeded in 96-well plates. After 1–4 days, 10 μl of CCK-8 solution was added to each well, and the plates were incubated for 1 h at 37 °C. The optical density (OD) levels were measured by a microplate reader scanning at 450 nm according to the manufacturer's instructions.

Colony formation

2 × 10⁵ cells/well U251 and U87 cells were seeded on the 12-well plate and treated with USP39-siRNA or scramble-siRNA for 48 h. Cells were trypsinized, centrifuged and diluted to 500/ml with DMEM

containing 10% FBS, and 1 ml cell suspensions were seeded in 6-well plates. After 10 days, cells were fixed with 4% paraformaldehyde and stained with crystal violet (Solarbio, Beijing, China).

Cell apoptosis assay

2 × 10⁵ cells/well U251 and U87 cells were seeded into 12-well plates treated with USP39-siRNA or scramble-siRNA for 24 h, adherent cells were treated with serum free medium for another 48 h to induce cells apoptosis. Cells were trypsinized, centrifuged, washed with ice-cold PBS buffer. The apoptosis of cells was detected by flow cytometry (FCM) with an Annexin V-FITC/propidium iodide (PI) apoptosis detection kit (BD Biosciences, San Jose, CA, USA) according to the manufacturer's instructions. Briefly, resuspending cells with 100 μl binding buffer, then cells were incubated in 5 μl PI staining solution and 5 μl Annexin V-FITC for 15 min at RT in the dark. The apoptotic cells were determined using a flow cytometer (FACSCalibur; BD Biosciences). Each sample had 3 repetitions. Both early and late apoptotic cells were included in cell apoptotic determinations.

Cell cycle assay

2 × 10⁵ U251 or U87 cells were incubated into 12-well plates, adherent cells were treated with serum-free medium for 24 h to keep cells in the same period, continuing to cultivate 48 h after siRNA interference treatment. Cells were treated with trypsin and centrifuged in 300 g for 5 min. After suspending in PBS and centrifuging in 300 g for 5 min, cells were suspended and fixed with 1 ml 70% cold ethanol at 4 °C for overnight. Then centrifuging in 800 g for 5 min at 4 °C and suspending with 1 ml PBS buffer containing 10% serum. After centrifuging in 800 g for 5 min at 4 °C again and adding 500 μl PI/RNase A staining buffer (BD Biosciences), cells were incubated at RT for 30 min in the dark. Cell cycle data were obtained using a flow cytometer. The percentages of cells at the G₀/G₁, G₂/M and S phases were analyzed.

Tumor xenograft

U251 cells with stable knockdown USP39 labeled by GFP (Green Fluorescent Protein) (U251-shUSP39 cells) or U251-shNC cells with GFP (5 × 10⁶ /100 μl) were injected into athymic BALB/c nude mice (6–8 weeks old, Guangdong Medical Laboratory Animal Center, China) by subcutaneous injection. Tumors were measured every 3 days using a Vernier caliper, and the volume was determined using the formula $V = ab^2/2$ (a = length of tumor, b = width of tumor). Fluorescent images were captured using an IVIS Spectrum imaging system at the 21 days post-tumor cells injection. For the orthotopic xenograft mouse model, the detail methods were described in our previous study [12]. Briefly, U87-OE-Con and U87-OE-USP39 cells (5 × 10⁵/4 μl) were injected through an entry site at the bregma 2 mm to the right of the sagittal suture and 3 mm below the surface of the skull of anesthetized mice using a stereotactic apparatus (RWD Life Science, Shenzhen, China). Past inoculated of tumor cells 21 days, the mice were sacrificed, the tumors were weighed and then homogenate for the analysis of USP39 and Cyclin B1 protein expression by immunoblotting. If necessary, mice were systemic perfused with saline solution and 4% paraformaldehyde, and stripped brain tissues were prepared for H&E (Hematoxylin-eosin) and immunohistochemistry (IHC) staining. The animal experimental manipulation was performed according to the National Institute of Health Guide for the Care and Use of Laboratory Animals, with the approval of the animal ethical and welfare committee of the Shenzhen University (Approval number: AEW-2,021,009).

Statistical analysis

Data are presented as the mean ± SD or mean ± SEM. At least three independent experiments were applied in each group. Statistical

analyses were performed with the Student's *t*-tests or Two-way ANOVA. P value < 0.05 (95% confidence interval) was statistically significant. Statistical significance is represented in figures by: **p* < 0.05, ***p* < 0.01, ****p* < 0.001. Survival curves were estimated for each group, considered separately, using the Kaplan-Meier method, and compared statistically using the log rank test. A two-sided χ^2 -test and Fisher's exact test were both used to determine the association between USP39 and Cyclin B1. Data analysis was conducted using GraphPad Prism 7 software (GraphPad Software, San Diego, CA, USA).

Results

USP39 stabilizes Cyclin B1 protein level

Abnormal expression of Cyclin B1 in various of tumors could be regulated by ubiquitination and deubiquitination. To explore the deubiquitinase of Cyclin B1 in human glioma, we first analyzed the expression level of all ubiquitin-specific protease (USP) family proteins in human glioma samples from TCGA (The Cancer Genome Atlas) database [14]. The top 7 genes of USPs (*USP1*, *USP3*, *USP10*, *USP18*, *USP38*, *USP39*, *USP41*) with highest expression difference between the normal samples and GBM samples and the expression of Cyclin B1

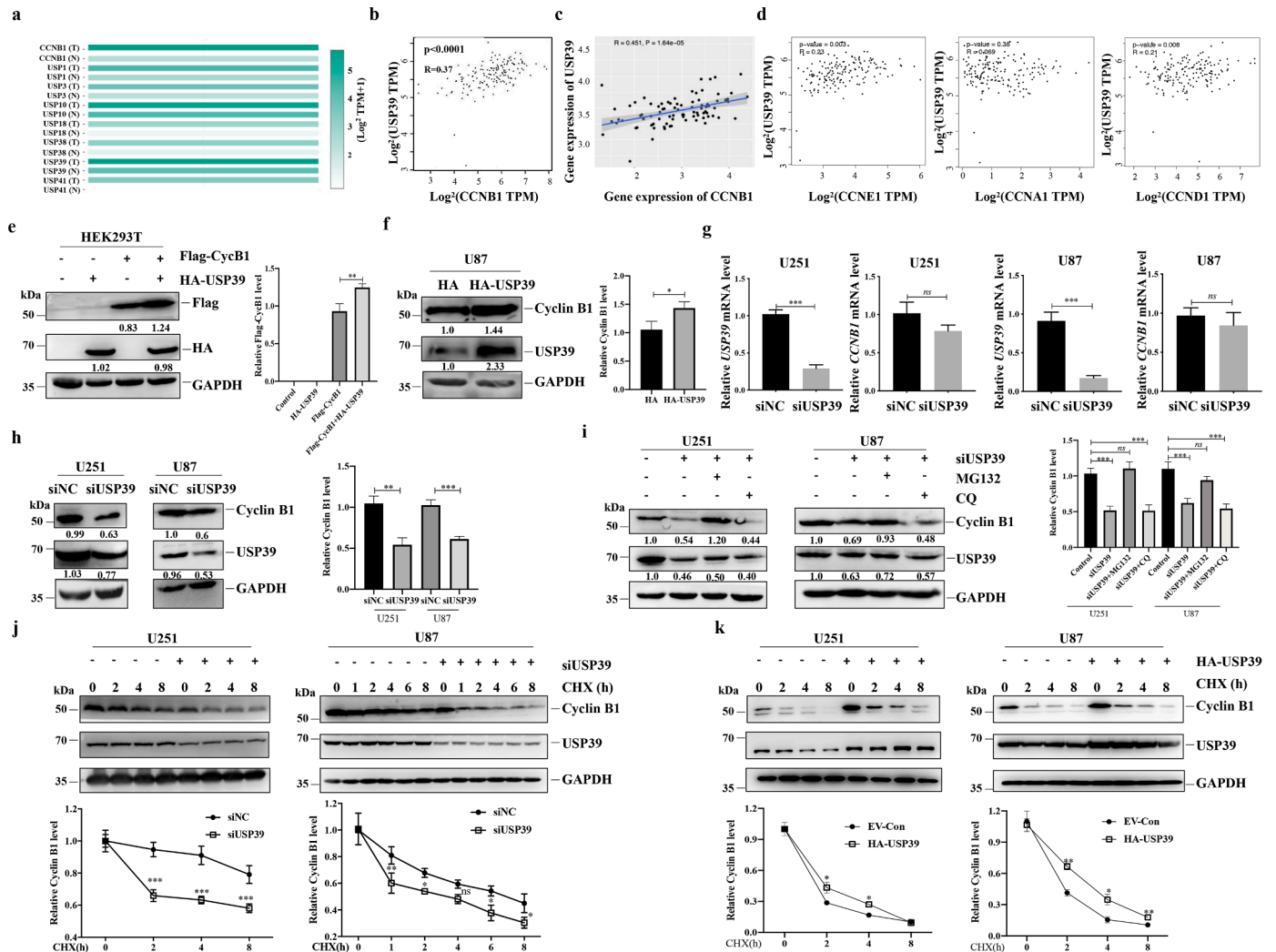


Fig. 1. USP39 regulates Cyclin B1 protein level. (a) Heatmap analysis of the expression levels of CCNB1 and USP1, USP3, USP10, USP18, USP38, USP39, USP41 in TCGA GBM and normal samples from GEPIA databases. T, tumor samples; N, normal samples. (b) Statistical analysis of the correlation analysis between CCNB1 and USP39 expression of TCGA GBM samples from GEPIA databases (*P*<0.001, *R* = 0.37). (c) Statistical analysis of the correlation analysis between CCNB1 and USP39 expression of WHO IV glioma samples from CGGA databases (*P*<0.001, *R* = 0.451). (d) Statistical analysis of the correlation analysis between CCNE1, CCNA1, CCND1 and USP39 expression of TCGA GBM samples from GEPIA databases. (e) HEK293T cells were transfected with Flag tagged Cyclin B1 (Flag-CycB1) and HA tagged USP39 (HA-USP39) plasmid. After 30 h, cells were lysed, and the lysates were immunoblotted with the indicated antibodies. (f) U87 cells were transfected with HA tag vector or HA-USP39 plasmid for 30 h, cell lysates were immunoblotted with the indicated antibodies. (g) U251 and U87 cells were transfected with control siRNA (siNC) or USP39 siRNA (siUSP39) for 48 h, qPCR analyzed the mRNA levels of USP39 and Cyclin B1. (h) U251 and U87 cells were transfected with control siRNA (siNC) or USP39 siRNA (siUSP39) for 72 h, cell lysates were immunoblotted with the indicated antibodies. (i) U251 and U87 cells were transfected with siNC or siUSP39 for 60 h, followed by MG132 (20 μ M) or Chloroquine (50 μ M) treatment for 6 h. Cell lysates were immunoblotted with the indicated antibodies. (j) U251 and U87 cells were transfected with siNC or siUSP39 for 60 h, followed by cycloheximide (100 μ g/ml) treatment for the indicated times. The cell lysates were immunoblotted with the indicated antibodies (upper panels). A plot of the Cyclin B1 level relative to GAPDH is shown (lower panels). (k) U251 and U87 cells were transfected with empty vector plasmid (EV) or HA-USP39 for 24 h, followed by cycloheximide (100 μ g/ml) treatment for the indicated times. The cell lysates were immunoblotted with the indicated antibodies (upper panels). A plot of the Cyclin B1 level relative to GAPDH is shown (lower panels). The data were from three repeated experiments. Bars represent means \pm SEM. Student's-test, ns, no significance, **p* < 0.05, ***p* < 0.01, ****p* < 0.001.

(CCNB1) were shown in Fig. S1a and 1a. Then, we analyzed the correlation between the *USPs* expression and *CCNB1* expression in GBM samples from GEPIA database, the results indicated that *USP1*, *USP39* and *USP41* expression were significantly positively correlated with *CCNB1* expression (Fig. 1b and S1b). As the deubiquitinating activity of *USP39* was controversial, we further study the role of *USP39* in regulating Cyclin B1 expression. The positive correlation between *USP39* expression and *CCNB1* expression in WHO IV glioma were further confirmed in the database derived from the Chinese Glioma Genome Atlas (CGGA) (Fig. 1c). Besides, we analyzed the correlation *CCNA1*, *CCND1* and *CCNE1* expression with *USP39*, the correlation data were

showed that *CCNB1* indeed have the strongest correlation to *USP39* (Fig. 1d). In HEK293T and U87 cells, overexpression of *USP39* could increase Cyclin B1 protein level (Fig. 1e and f). On the other hand, we knocked down *USP39* using specific siRNA in U87 and U251 cells and then detected Cyclin B1 protein level. We found that knockdown of *USP39* could not influence the mRNA levels of Cyclin B1 but decreased the expression level of Cyclin B1 (Fig. 1g and h). Moreover, in other human tumor cell lines, such as A549, MDA-MB-231 and SW480, knockdown of *USP39* could also downregulate Cyclin B1 expression (Fig. S2). Protein degradation mainly had two pathways, one is proteasome-dependent manner, and another is lysosome-dependent

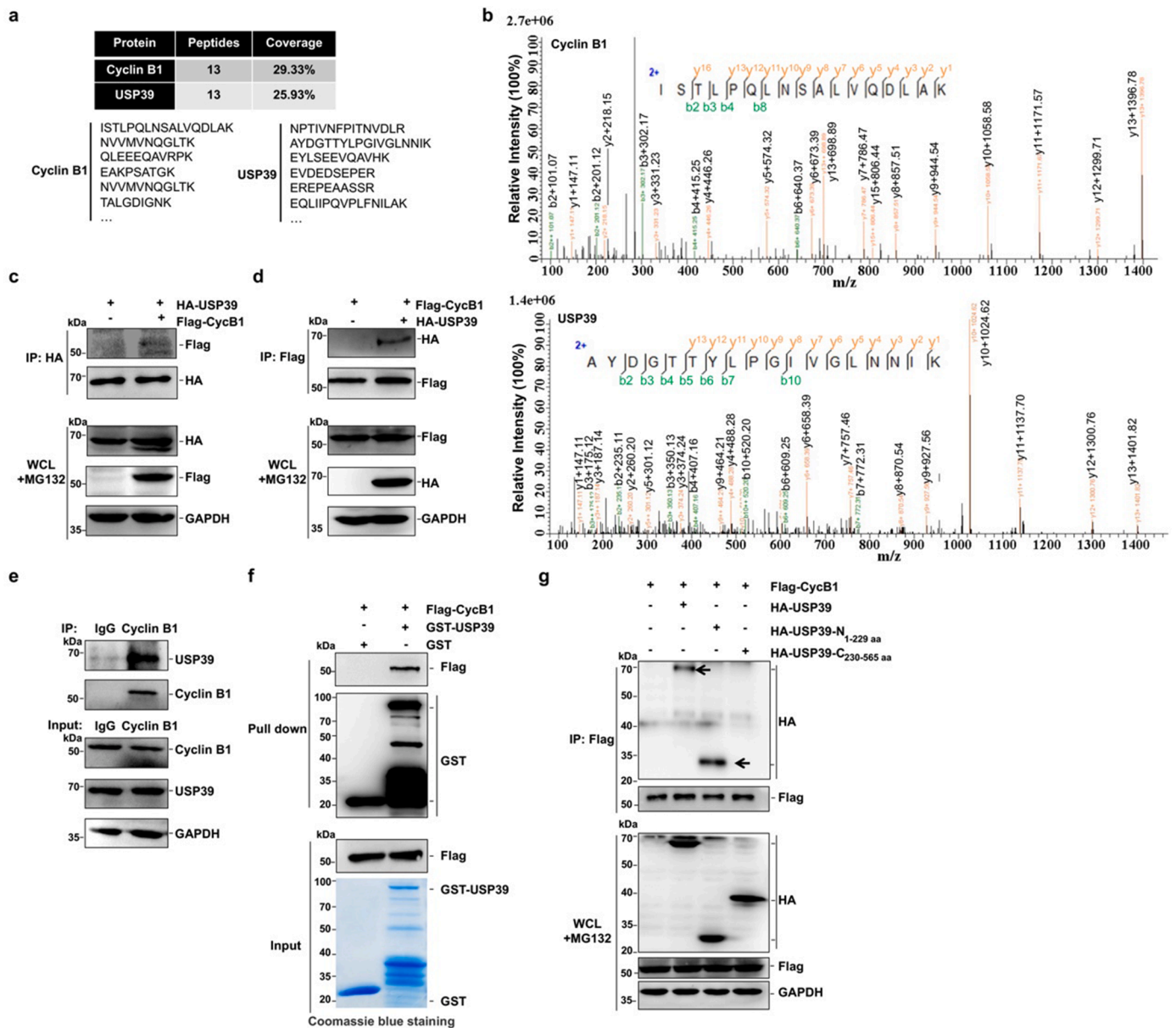


Fig. 2. USP39 directly interacts with Cyclin B1. (a, b) The proteins from the Flag-CycB1 transfected HEK293T cells were precipitated using Flag-M2 beads and subjected to MS analysis. Peptide coverage and representative peptide fragments are shown. The MS/MS spectrum corresponding to ISTLPQLNSALVADLAK of Cyclin B1 and AYDGTTYLPGIVGLNNIK of USP39 are shown. Observed b- and y-ion series are indicated. (c, d) HEK293T cells co-transfected with HA-USP39 and Flag-CycB1 plasmids followed by immunoprecipitation using antibody to HA tag (c) or Flag-M2 beads (d), and then the immunocomplexes were analysed by immunoblotting. All cells were treated with MG132 (20 μM), a membrane-permeable proteasome inhibitor. (e) Endogenous USP39 proteins were immunoprecipitated with anti-Cyclin B1 antibody or IgG, and then the immunocomplexes were analysed by immunoblotting. (f) HEK293T cell transfected with Flag-CycB1, and then cell lysates were incubated with Sepharose coupled with GST or GST-USP39 for 2 h at 4 °C, after washing, proteins bound on Sepharose were immunoblotted with indicated antibodies. The input GST and GST-USP39 protein were analysed by Coomassie blue staining. (g) HEK293T cells were co-transfected Flag-CycB1 with empty vector, HA-USP39, HA-USP39-N (1–229 aa) or HA-USP39-C (230–565 aa) plasmids followed by immunoprecipitation using Flag-M2 beads, and immunocomplexes were analyzed by immunoblotting. All cells were treated with MG132 (20 μM). WCL, whole cell lysis.

manner. To investigate the manner involved in USP39 stabilizing expression of Cyclin B1, we transfected USP39 siRNA into U251 and U87 cells, then treated with proteasome inhibitor MG132 or lysosome inhibitor chloroquine (CQ). Immunoblot analysis demonstrated that only MG132 rescued the degradation of Cyclin B1 upon USP39 knockdown (Fig. 1i), this result suggested USP39 stabilized expression of Cyclin B1 in proteasome-dependent manner. A cycloheximide (CHX) chase assay in U251 and U87 cells showed that knockdown of USP39 decreased the half-life of Cyclin B1 (Fig. 1j), and upregulation of USP39 increased the half-life of Cyclin B1 (Fig. 1k). Taken together, these results suggest that USP39 knockdown promotes Cyclin B1 protein degradation in a proteasome-dependent manner.

USP39 directly interacts with Cyclin B1

Next, we sought to detect an interaction of Cyclin B1 and USP39. Whole-cell extracts from HEK293T cells with Flag-Cyclin B1 (Flag-CycB1) expression was applied to immunoprecipitation and mass spectrometry (MS) analysis. By this approach, we found USP39 as a Cyclin B1-binding protein in precipitates of Flag-CycB1. Thirteen specific peptides corresponding to human USP39 were detected, as illustrated by a representative MS/MS spectrum corresponding to ²¹⁴AYDGTTYLP-GIVGLNNIK²³¹ is shown in Fig. 2a and b. To confirm our MS findings, we transfected HEK293T cells with Flag-CycB1 and HA-USP39 expression plasmids. Cell lysates were immunoprecipitated using anti-HA antibody or Flag-M2 beads. Anti-HA immunoprecipitated Flag-CycB1 and Flag-M2 immunoprecipitated HA-USP39, suggesting that USP39 and Cyclin B1 physically interact (Fig. 2c and d). Additionally, the interaction between endogenous USP39 and Cyclin B1 in U87 cells was demonstrated by anti-Cyclin B1 immunoprecipitation (Fig. 2e). To test whether the Cyclin B1-USP39 interaction was direct, we performed GST-pull down assays using GST-USP39 and Flag-CycB1. The results further revealed that USP39 directly binds to Cyclin B1 (Fig. 2f). We then generated two truncated domains of USP39 to delineate the regions within the USP39 protein essential for its interaction with Cyclin B1. The results of co-immunoprecipitation assay indicated that the N-terminus (aa1–219) of USP39 displayed a capability to interact with Cyclin B1 (Fig. 2g). Collectively, these results indicate that USP39 directly interacts with Cyclin B1.

USP39 reverses K29-linked polyubiquitination of Cyclin B1 at K242

To understand the functional significance of the interaction between USP39 and Cyclin B1, we assessed whether USP39 deubiquitinates Cyclin B1 in cells. As shown in Fig. 3a, overexpressing USP39 in HEK293T cells resulted in a significant decrease in polyubiquitination of Cyclin B1. Conversely, knockdown of USP39 in U87 cells increased the endogenous ubiquitination levels of Cyclin B1 (Fig. 3b). The endogenous ubiquitination levels of Cyclin B1 was also increased in the A549, MDA-MB-231 and SW480 cells transfected with USP39 siRNA (Fig. S3). Furthermore, to investigate the form of ubiquitination chains linked to Cyclin B1, HEK293T cells co-transfected with Flag-CycB1, Myc-USP39 and each one of the different ubiquitins (HA-tagged K6, K11, K27, K29, K33, K48 or K63-ubiquitin, individual ubiquitin constructs could only form ubiquitin linkages at a single lysine) were performed a co-immunoprecipitation assay using anti-Flag-M2 beads. The result showed that compared to other HA-Kn-Ubs, the expression level of HA-K29-Ub was downregulated by adding the Myc-USP39 plasmid in the cells (Fig. 3c). To confirm that USP39 directly deubiquitinates the K29-linked ubiquitination of Cyclin B1, we co-expressed His-Cyclin B1 with HA-K29-Ub in HEK293T cells. Cyclin B1 proteins containing K29-linked conjugates was pull down using Ni-NAT agarose followed by elution with elution buffer containing imidazole. The eluate was sequentially incubated with GST-USP39 protein or GST protein followed by detection of K29 linked-CycB1 using anti-HA antibody with Western blotting. The result showed that the K29-linked ubiquitination of Cyclin B1 was

significantly reducible after incubated with GST-USP39 protein, suggesting that USP39 directly deubiquitinates Cyclin B1 (Fig. 3d). Furthermore, we proved that USP39 deubiquitinated the K29-linked Ub of Cyclin B1 in a dose-dependent manner (Fig. 3e). Previous functional study indicated that the C306 site is important for the deubiquitinating enzymic activity of USP39 [15]. Thus, we constructed a USP39 C306A (enzyme inactive mutant) mutant plasmid to further confirm the deubiquitination effect of USP39 on Cyclin B1. Co-immunoprecipitation experiments analysis demonstrated that USP39 mutant C306A failed to cleave ubiquitin chains or K29-linked polyubiquitin chains from Cyclin B1 (Fig. 3f and g). Altogether, these results indicate that USP39 deubiquitylates the K29-linked polyubiquitin chains of Cyclin B1.

We next constructed a series of expression vectors encoding Cyclin B1 mutants in which lysine (K) residues that might be ubiquitinated were replaced with arginine (R), then assessed their ubiquitination levels affected by Myc-USP39 in HEK293T cells. Among the Cyclin B1 mutants we constructed, only the ubiquitination of K242R mutant was not reduced by the Myc-USP39 (Fig. 3h). Identically, USP39 failed to deubiquitinate the K29-linked Ub of Cyclin B1 K242R mutant (Fig. 3i). To investigate whether USP39 regulates Cyclin B1 K242R mutant protein stability, we co-transfected Flag-CycB1 K242 plasmid and HA-USP39 into HEK293T cells and then performed a Western blotting assay. The result showed that USP39 failed to upregulate the expression of K242R mutant, compared to the expression of Cyclin B1 wild type (WT) protein (Fig. 3j). Furthermore, the site of Cyclin B1 at K242 is conserved in mammals (Fig. 3k). Taken together, these data indicate that USP39 cleaves K29-linked Ub chains of Cyclin B1 at K242 site.

USP39 promotes glioma cells proliferation via Cyclin B1

Cyclin B1 expression regulates the development of various human tumors. Hence, it is possible that USP39 could regulate the functions of Cyclin B1 via deubiquitinating and stabilizing it. To test this hypothesis, glioma cells with USP39 siRNA transfection were employed to detect cell proliferation, apoptosis and cell cycle. As shown in Fig. 4a, knockdown of USP39 significantly inhibited the U251 cells proliferation at 48 h, 72 h and 96 h ($p < 0.001$) and inhibited the growth of U87 cells at 72 h and 96 h ($p < 0.001$). Besides, knockdown of USP39 also inhibited the cell proliferations of A549, MDA-MB-231 and SW480 (Fig. S4a). To quantify the clonogenic capacity of U251 and U87 cells with USP39 siRNA transfection, a colony formation assay was performed, and the results showed that the clone number of U251 and U87 cells treated with USP39 siRNA was significantly decreased compared to the control-scramble siRNA transfection (Fig. 4b). Additionally, flow cytometry was used to detect the apoptosis and cell cycle of U251 and U87 cells transfected with USP39 siRNA. As shown in Fig. 4c, the percentage of total Annexin⁺ cells (Annexin⁺PI⁺ cells plus Annexin⁺PI⁻ cells) in U251-siUSP39 cells or U87-siUSP39 cells increased nearly 0.8-fold or 0.5-fold compared to that in U251-siNC cells or U87-siUSP39, respectively. We also found that knockdown of USP39 could increase the percentage of cells in G2/M transition in U251, U87, A549, MDA-MB-231 and SW480 cells (Fig. 4d and Fig. S4b). Besides, we treated U87 cells with CDK1 inhibitor RO-3306 (9 μ m) for 24 h to synchronize the cells at the G2/M border, then collected the cells expressing siNC or siUSP39 for 48 h and 72 h. Flow cytometry showed that knocking down USP39 leads to the increase of cells in G2/M phase, as shown in Fig. S5. As that the Cyclin B1 promotes cell cycle transition from G2 to M phase, we assessed whether overexpression of Cyclin B1 rescued cell proliferation, colony formation and cell cycle to identify whether the effect of USP39 on promoting glioma cells proliferation was dependent on Cyclin B1. The overexpression level of Cyclin B1 in U87 cells expressing USP39 siRNA was checked by immunoblotting with Cyclin B1 antibody (Figure S6). In a CCK-8 assay, we found that Cyclin B1 could rescue U87 cells proliferation induced upon USP39 knockdown (Fig. 4e). Besides, the colony numbers in U87-siUSP39 cells with Cyclin B1 were increased approximately 0.8-fold compared with that in U87-siUSP39 cells with

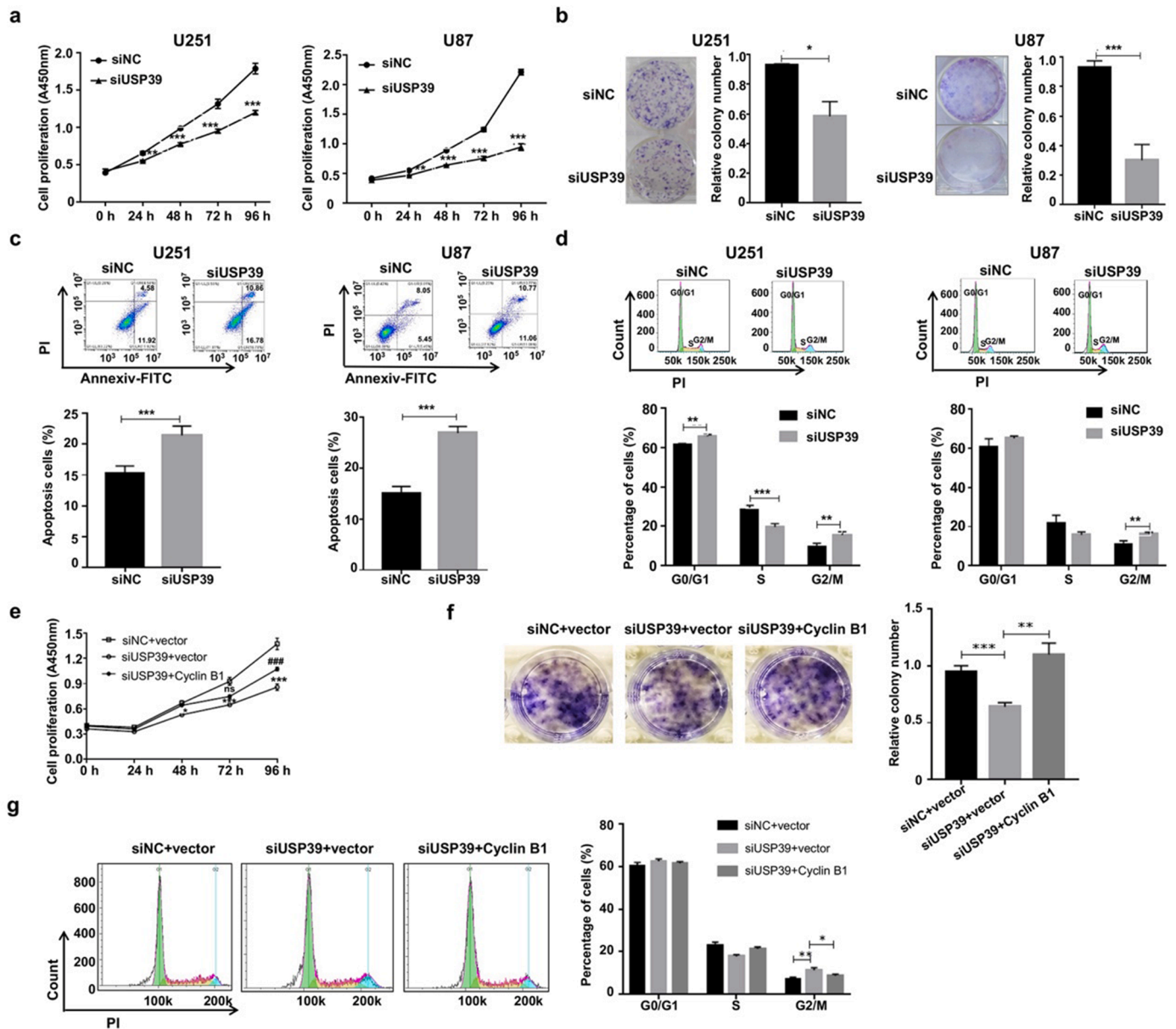
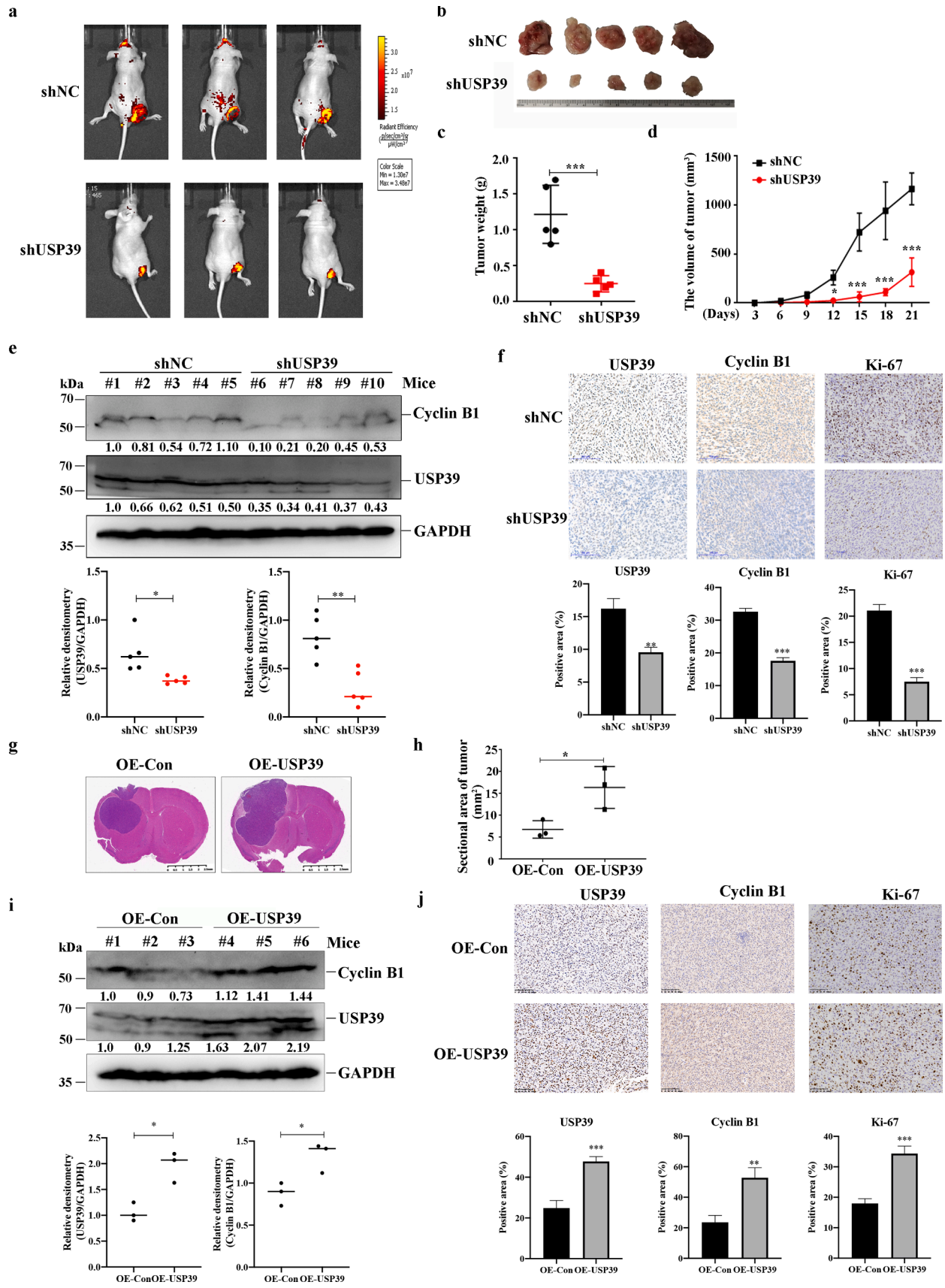


Fig. 4. USP39 promotes glioma cells proliferation via Cyclin B1. (a) Cell Counting Kit-8 (CCK-8) assay was used to detect the viability of U251 and U87 cells transfected with negative control siRNA (siNC) or USP39 siRNA (siUSP39). Two-way ANOVA test, $**p < 0.01$, $***p < 0.001$. (b) Colony formation assay was used to determine the clonogenic capacity of U251 and U87 cells transfected with siNC or siUSP39. Cells were fixed and stained with Giemsa Stain solution. Graphical representations of relative colony number of cells were presented. $*p < 0.05$, $***p < 0.001$. (c) Flow cytometry analysis of the apoptosis of U251 and U87 cells transfected with siNC or siUSP39 using Annexin V and propidium iodide (PI) staining. Graphical representations of percentages of total Annexin V-positive cells were presented. $***p < 0.001$. (d) Flow cytometry analysis of the cell cycle of U251 and U87 cells transfected with siNC or siUSP39 using PI staining. Graphical representations of percentages of cells in G0/G1, S, and G2/M phase were presented. $**p < 0.01$, $***p < 0.001$. (e-f) U87 cells expressing the control siRNA (siNC) or USP39 siRNA (siUSP39) were transfected with Flag-CycB1 (Cyclin B1) or Flag-tagged empty vector (vector). (e) CCK-8 assay was performed to detect the viability of the U87 cells. Two-way ANOVA test, $**p < 0.01$, $***p < 0.001$ vs. siNC+vector, $##p < 0.01$, $###p < 0.001$ vs. siUSP39+Cyclin B1. (f) Colony formation assay was used to determine the clonogenic capacity of the U87 cells. Cells were fixed and stained with Giemsa Stain solution. Graphical representations of relative colony number of cells were presented. $**p < 0.01$, $***p < 0.001$. (g) Flow cytometry analysis of the cell cycle of the U87 cells using PI staining. Graphical representations of percentages of cells in G0/G1, S, and G2/M phase were presented. $**p < 0.01$, $***p < 0.001$. (b-d, f-g) The statistics are shown as mean \pm SD, with p values determined by Student's t -test (two tail). The data are from one experiment representative of three independent experiments with similar results.

empty vector (Fig. 4f). Furthermore, over-expressed Cyclin B1 delayed cell cycle progression at G2/M transition induced by knockdown of USP39 in U87 cells (Fig. 4g). Collectively, over-expressed Cyclin B1 could rescue the decreased potential of cells proliferation, colony formation and cell cycle progression at G2/M transition induced by knockdown of USP39.

USP39 promotes the progression of glioma xenografts in nude mice

To assess the effects of USP39 in the progression of glioma *in vivo*, GFP-labeled U251 cells expressing USP39 shRNA were injected into the flanks of BALB/c nude mice. At 21 days post-cells injection, the green fluorescence signals in shUSP39-U251 tumor were markedly lower than that in negative control shRNA (shNC) U251 tumor (Fig. 5a). The tumor size and weight of shUSP39-U251 were obviously smaller than that of



(caption on next page)

Fig. 5. USP39 promotes the progression of glioma in nude mice xenografts. (a-f) BALB/c nude mice were subcutaneously injected with U251 cells stably expressed GFP-labeled USP39 shRNA (shUSP39) or negative control shRNA (shNC). (a) Representative image of fluorescence signals in mice at days 21 post tumor cell injection by a live imaging system. (b) The photo of tumor isolated from the mice at days 21 post tumor cell injection. (c) Tumor weight were measured at days 21 post tumor cell injection. $n = 5$ mice/group, error bars represent mean \pm SD, $***p < 0.001$, Student's *t*-test (two tail). (d) Tumor volumes were measured every 3 days. $n = 5$ mice/group, error bars represent mean \pm SD, $***p < 0.001$, Two-way ANOVA. (e) Tumor tissue lysates were immunoblotted with the indicated antibodies for analyzing the expression of USP39 and Cyclin B1 in tumor. $n = 5$ mice/group, error bars represent mean \pm SD, Student's *t*-test (two tail), $*p < 0.05$, $**p < 0.01$. (f) IHC analysis of USP39, Cyclin B1 and Ki-67 in tumors tissues. Representative images are shown. Scale bar, 100 μ m. Graphical representations of the positive area were presented. error bars represent mean \pm SD, Student's *t*-test (two tail), $**p < 0.01$, $***p < 0.001$. (g-j) BALB/c nude mice were intracranially injected with U87 cells stably expressed USP39-overexpressed plasmid (OE-USP39) or negative control plasmid (OE-Con). (g) Hematoxylin-eosin (H&E) staining of orthotopic xenografts derived from the indicated U87-OE-USP39 cells and control in nude mice ($n = 3$ /group). Representative images are shown. Scale bar: 2.5 mm (as indicated in the picture). (h) Sectional area of tumor was measured at days 20 post tumor cell injection. $n = 3$ mice/group, error bars represent mean \pm SD, $*p < 0.05$, Student's *t*-test (two tail). (i) Tumor tissue lysates were immunoblotted with the indicated antibodies for analyzing the expression of USP39 and Cyclin B1 in tumor. $n = 3$ mice/group, error bars represent mean \pm SD, $*p < 0.05$, Student's *t*-test (two tail). (j) IHC analysis of USP39, Cyclin B1 and Ki-67 in tumors tissues. Representative images are shown. Scale bar, 100 μ m. Graphical representations of the positive area were presented. error bars represent mean \pm SD, $**p < 0.01$, $***p < 0.001$, Student's *t*-test (two tail).

shNC U251 (Fig. 5b and c). The tumor size was measured every three days after tumor cell injection. The data showed that the growth of U251 glioma transfected with USP39 shRNA were significantly lower than that shNC U251 glioma (Fig. 5d). The western blotting analyses demonstrated that USP39 and Cyclin B1 levels were downregulated in the shUSP39 U251 cells (Fig. 5e). In addition, USP39 silencing in U251 cells exhibited decreased Cyclin B1 protein levels and the number of Ki67 positive tumor cells by IHC analyses (Fig. 5f).

Further on, U87 cells were infected with lentivirus vector carrying USP39 cDNA to establish a stably U87 cell expressing USP39 protein. The USP39 overexpressing U87 cells (OE-USP39) or control U87 cells (OE-Con) were intracranially implanted into the brains of BALB/c nude mice. H&E (Hematoxylin-eosin) staining analyses and the measured tumor area showed that USP39 promoted the growth of U87 tumor *in vivo* (Fig. 5g and h). Western blotting analyses demonstrated that USP39 and Cyclin B1 levels were upregulated in the OE-USP39 U87 cells (Fig. 5i). In addition, USP39-overexpressed U87 cells exhibited increased Cyclin B1 protein levels and the number of Ki67 positive tumor cells by IHC analyses (Fig. 5j).

USP39 expression positively correlates with Cyclin B1 in human tumors

To further confirm the correlation between USP39 and Cyclin B1, we analyzed the clinical data of human glioma tissue microarrays (TMA) from the Department of Neurosurgery of the Second Affiliated Hospital, Zhejiang University, School of Medicine (Hangzhou, China) and TCGA tumor samples from GEPIA databases. Immunohistochemistry was performed on the TMA using USP39 and Cyclin B1 antibodies, respectively (Fig. 6a). As shown in Fig. 6b and c, the USP39 and Cyclin B1 expression levels in WHO grades I-II glioma and WHO grades III-IV glioma were higher than that in normal tissues. Besides, in the glioma TMA samples, the expression of USP39 was positively correlated with Cyclin B1 expression (Fig. 6a and d). Furthermore, we detected the USP39 and Cyclin B1 levels in the glioma tissues derived from patients by western blotting. The results showed that the glioma tissues expressing highly USP39 protein were also exhibited high Cyclin B1 levels, especially the #3 sample. Consistently, the glioma tissues expressing lowly USP39 protein were also exhibited low Cyclin B1 levels, especially the #4 sample (Fig. 6e). Finally, we analyzed the correlation between the USP39 expression and CCNB1 expression in glioblastoma multiforme (GBM), low grade glioma (LGG), lung squamous cell carcinoma (LUAD), stomach adenocarcinoma (STAD), colon adenocarcinoma (COAD), liver hepatocellular carcinoma (LIHC), ovarian serous cystadenocarcinoma (OV) and breast invasive carcinoma (BRCA) from GEPIA database, the results indicated that USP39 expression was significantly positively correlated with Cyclin B1 expression (Fig. 6f). Taken together, these results suggest that USP39 expression positively correlates with Cyclin B1 in human glioma and other human tumors. Finally, we analyzed the correlation of USP39 and Cyclin B1 expression to patient prognosis in the CGGA databases. The data shown that patients with high expression

of USP39 and Cyclin B1 had shorter overall survival than those with low expression (Fig. 6g and h).

Discussion

Glioma, in particular glioblastoma multiforme (GBM), is the most common and lethal malignant primary brain tumor in adults [16,17]. Despite current advances in multimodality therapy for GBM involving surgical resection, radiation, and chemotherapy, the long-term survival is rare and postoperative recurrence is common [18]. Significant progress in the understanding of the molecular pathology of GBM has provided opportunities for new treatments for recurrent and newly diagnosed disease. Here, we showed that ubiquitin-specific protease 39 (USP39) promoted glioma cell proliferation *in vitro* and the growth of orthotopic glioma *in vivo*. We reported similar results in our previous study, in which knockdown of USP39 suppressed the glioma cell migration and invasion *in vitro* and inhibited glioma growth and invasion *in vivo* [12]. Besides, Ding et al. firstly reported that USP39 acted as an oncogene to promote glioma progression and provided a new therapeutic target for glioma [19]. Whereas, in their study and our previous study, USP39 functioned as an RNA splicing factor to regulate TAZ or ADAM9 mRNA maturation, promoting glioma progression [12,19]. Here, we explore a novel molecular mechanism of USP39 on the regulation of glioma progression. USP39 was identified as a new deubiquitinating enzyme of Cyclin B1 which stabilizes its expression, facilitating the cell cycle at G2/M transition and glioma cell proliferation. However, co-expressing Cyclin B1 failed to rescue the accelerated apoptosis of glioma cells induced by the downregulation of USP39 in glioma cells, suggesting the Cyclin B1 only affect the cell proliferation by regulating the cell cycle (data not shown). Besides, the expression of SOX2, a molecular marker of glioma stem cells, was reduced in the U251 cells transfected with USP39 siRNA (data not shown), indicating USP39 might also inhibit the stemness of glioma cells. In the present study, we used U251 and U87 glioma cell lines, which could not completely represent the low-passage GBM patient cells, to demonstrate the effect of USP39/Cyclin B1 on the cell proliferation. This was a limitation to the studies. To better reflect the relationship between USP39 and Cyclin B1 expression in clinical glioma patients, the TMA and tumor samples derived from glioma patients were used to further prove that USP39 and Cyclin B1 were highly expressed in glioma tissues with positive correlation. Meanwhile, patients with high expression of USP39 and Cyclin B1 had a poor prognosis.

Increasing evidence have shown that USP39 acted as an RNA splicing factor to participate in the development of normal cells or tumor cells [12,20-22]. In this study, we also detected whether the Cyclin B1 mRNA maturation could be affected by the USP39 expression. The data showed that knockdown of USP39 did not change Cyclin B1 mRNA maturation in U251 cells (Fig. S7). In recent years, the deubiquitinating function of USP39 has raised great interest of scientists, both in innate immune response and cancer research [23]. In the development of hepatocellular

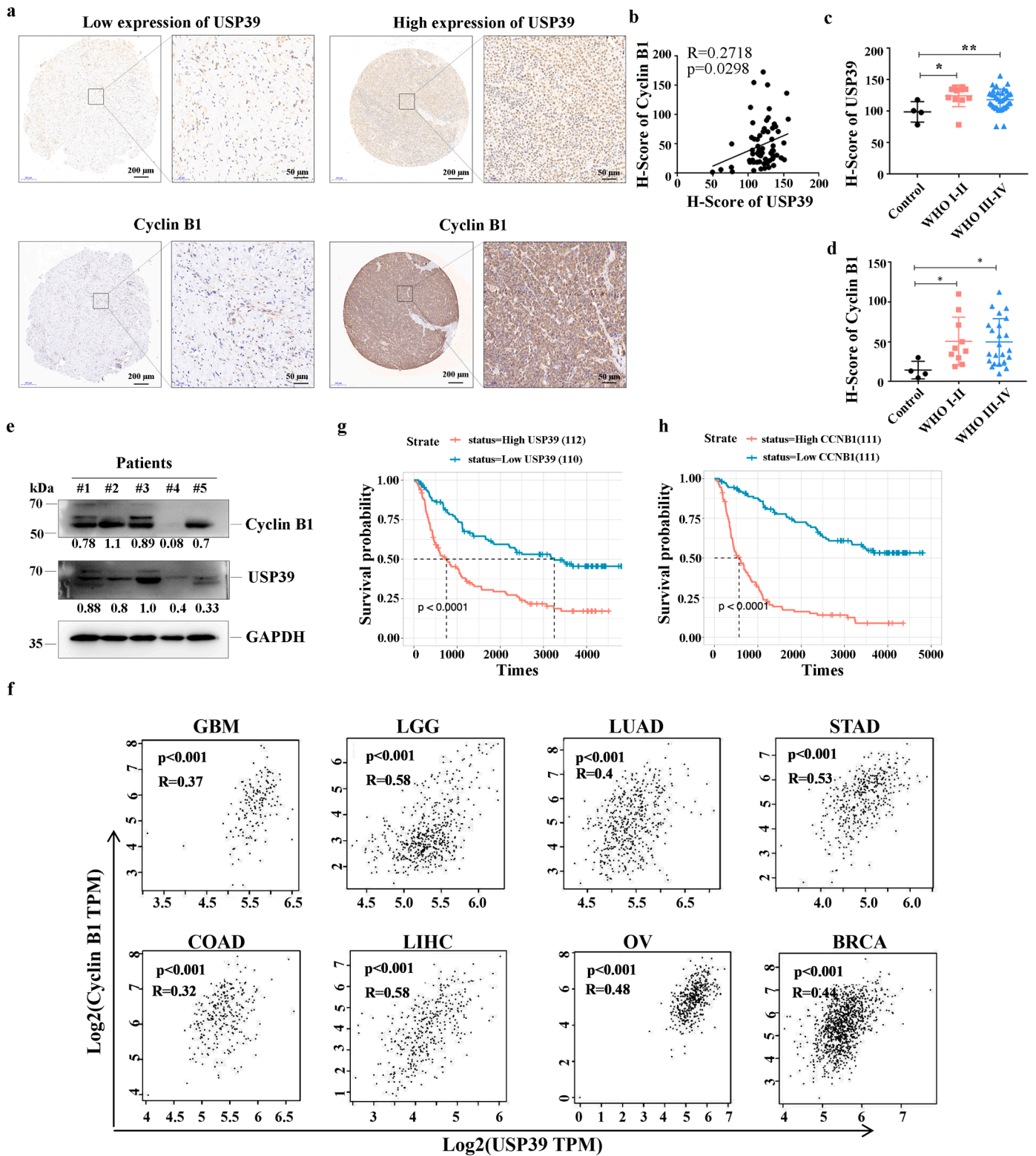


Fig. 6. USP39 expression positively correlates with Cyclin B1 in human tumors. (a) The expression levels of USP39 (upper) and Cyclin B1 (lower) in tissue microarrays (TMA) slides of paraffin-fixed human glioma tissue were determined by IHC with specific antibodies. (b) Statistical analysis of the correlation analysis between USP39 and Cyclin B1 expression in TMA ($n = 63$). (c) Graphical representation of the H-score of USP39 in normal tissue control, WHO grades I-II glioma and WHO grades III-IV glioma from human glioma tissues microarrays (TMA) ($n = 63$). $*p < 0.05$, $**p < 0.01$, $***p < 0.001$ Student's t -test. (d) Graphical representation of the H-score of Cyclin B1 in normal tissue control, WHO grades I-II glioma and WHO grades III-IV glioma from human glioma TMA ($n = 63$). $*p < 0.05$, $**p < 0.01$, $***p < 0.001$ Student's t -test. (e) Protein level of USP39 and Cyclin B1 in human glioma tissues detected by immunoblotting, and ratios of gray scale showing the difference in the picture. (f) Statistical analysis of the correlation analysis between Cyclin B1 and USP39 expression of TCGA GBM, LGG, LUAD, STAD, COAD, LIHC, OV and BRCA samples from GEPIA databases. (g) Overall survival curves of USP39 expression in glioma patients based on CGGA database. High group, $n = 112$; Low group, $n = 110$. (h) Overall survival curves of Cyclin B1 expression in glioma patients based on CGGA database. High group, $n = 111$; Low group, $n = 111$.

carcinoma, USP39 and E3 ligase TRIM26 balance of the ubiquitination level and stabilization of ZEB1 determines cell proliferation and migration [24]. Our findings that USP39 directly associated with and deubiquitinated Cyclin B1, provide a new evidence for the deubiquitinase catalytic activity of USP39.

Ubiquitination and its reversal process deubiquitination, play vital roles in the regulation of cell cycle [9]. Due to the central role of Cyclin B1 in cell cycle, the protein amount of Cyclin B1 is tightly regulated by post-translational modification such as ubiquitination and deubiquitination. Although it has been reported that USP22 and USP14 can cleave the ubiquitin chains from Cyclin B1 [10,25], the cleaved ubiquitin linkage type and lysine site of Cyclin B1 are still unclear. In this report, we demonstrated that USP39 cleaves the K29-linked polyubiquitin chain on Cyclin B1 at Lys242. For this atypical K29 linkage type, most of studies reported its proteasome-independent function, such as signal transduction [26], regulation of antiviral innate immunity [27,28], or Wnt/beta-catenin signaling regulation [29]. However, Itch/AIP4 was shown to target deltex for degradation by K29-linked polyubiquitin chain formation [30].

Previous studies showed that Cyclin B1 is overexpressed in glioma which positively correlated with pathologic grades [31]. In this study, we demonstrate USP39 directly associated with Cyclin B1 to cleave lysine (K) 29-linked ubiquitin (Ub) of Cyclin B1 at K242 site. Our findings suggest that USP39-Cyclin B1 axis may function as the potential therapeutic target for the treatment of human glioma.

Declaration of Competing Interest

The authors declare that they have no known competing financial interests or personal relationships that could have appeared to influence the work reported in this paper.

Funding

This work was supported by grants from the Shenzhen Science and Technology Innovation Commission grant (No. JCYJ20180507182253653, JCYJ20190808172201639), Guangdong Province Basic and Applied Basic Research Fund (No. 2022A1515111143).

Acknowledgements

The authors thank the Instrument Analysis Center of Shenzhen University for providing instrument support.

Supplementary materials

Supplementary material associated with this article can be found, in the online version, at [doi:10.1016/j.tranon.2023.101713](https://doi.org/10.1016/j.tranon.2023.101713).

References

- [1] E.A. Barnes, M. Kong, V. Ollendorff, D.J. Donoghue, Patched1 interacts with cyclin B1 to regulate cell cycle progression, *EMBO J.* 20 (2001) 2214–2223.
- [2] L.A. Porter, D.J. Donoghue, Cyclin B1 and CDK1: nuclear localization and upstream regulators, *Prog. Cell Cycle Res.* 5 (2003) 335–347.
- [3] S.J. Moon, J.H. Kim, S.H. Kong, C.S. Shin, Protein Expression of Cyclin B1, Transferrin Receptor, and Fibronectin Is Correlated with the Prognosis of Adrenal Cortical Carcinoma, *Endocrinol. Metab. (Seoul)* 35 (2020) 132–141.
- [4] E. Ersvaer, et al., Prognostic value of mitotic checkpoint protein BUB3, cyclin B1, and pituitary tumor-transforming 1 expression in prostate cancer, *Mod. Pathol.* 33 (2020) 905–915.
- [5] H.Y. Liu, et al., Acetylation of MORC2 by NAT10 regulates cell-cycle checkpoint control and resistance to DNA-damaging chemotherapy and radiotherapy in breast cancer, *Nucleic. Acids. Res.* 48 (2020) 3638–3656.
- [6] L. Ding, et al., CREPT/RPRD1B associates with Aurora B to regulate Cyclin B1 expression for accelerating the G2/M transition in gastric cancer, *Cell Death. Dis.* 9 (2018) 1172.
- [7] H. Feng, et al., RNA-binding motif protein 43 (RBM43) suppresses hepatocellular carcinoma progression through modulation of cyclin B1 expression, *Oncogene* 39 (2020) 5495–5506.
- [8] S. Zhang, et al., Molecular mechanism of APC/C activation by mitotic phosphorylation, *Nature* 533 (2016) 260–264.
- [9] F. Dang, L. Nie, W. Wei, Ubiquitin signaling in cell cycle control and tumorigenesis, *Cell Death Differ.* 28 (2021) 427–438.
- [10] B. Liu, et al., CyclinB1 deubiquitination by USP14 regulates cell cycle progression in breast cancer, *Pathol. Res. Pract.* 215 (2019), 152592.
- [11] D. Komander, M.J. Clague, S. Urbe, Breaking the chains: structure and function of the deubiquitinases, *Nat. Rev. Mol. Cell Biol.* 10 (2009) 550–563.
- [12] Y. Xiao, et al., Ubiquitin-specific peptidase 39 promotes human glioma cells migration and invasion by facilitating ADAM9 mRNA maturation, *Mol. Oncol.* 16 (2021) 388–404.
- [13] S. Mukherjee, et al., Deubiquitination of NLRP6 inflammasome by Cyld critically regulates intestinal inflammation, *Nat. Immunol.* 21 (2020) 626–635.
- [14] D.S. Chandrashekar, et al., UALCAN: A Portal for Facilitating Tumor Subgroup Gene Expression and Survival Analyses, *Neoplasia* 19 (2017) 649–658.
- [15] J. Wu, et al., USP39 regulates DNA damage response and chemo-radiation resistance by deubiquitinating and stabilizing CHK2, *Cancer Lett.* 449 (2019) 114–124.
- [16] M.E. Glioblastoma Davis, Overview of Disease and Treatment, *Clin. J. Oncol. Nurs.* 20 (2016) S2–S8.
- [17] A. Behin, K. Hoang-Xuan, A.F. Carpentier, J.Y. Delattre, Primary brain tumours in adults, *Lancet* 361 (2003) 323–331.
- [18] P.Y. Wen, D.A. Reardon, Neuro-oncology in 2015: Progress in glioma diagnosis, classification and treatment, *Nat. Rev. Neurol.* 12 (2016) 69–70.
- [19] K. Ding, et al., RNA splicing factor USP39 promotes glioma progression by inducing TAZ mRNA maturation, *Oncogene* 38 (2019) 6414–6428.
- [20] Y. Rios, S. Melmed, S. Lin, N.A. Liu, Zebrafish usp39 mutation leads to rb1 mRNA splicing defect and pituitary lineage expansion, *PLoS Genet.* 7 (2011), e1001271.
- [21] R.J. van Leuken, M.P. Luna-Vargas, T.K. Sixma, R.M. Wolthuis, R.H. Medema, Usp39 is essential for mitotic spindle checkpoint integrity and controls mRNA-levels of aurora B, *Cell Cycle* 7 (2008) 2710–2719.
- [22] Y. Huang, et al., Overexpression of USP39 predicts poor prognosis and promotes tumorigenesis of prostate cancer via promoting EGFR mRNA maturation and transcription elongation, *Oncotarget* 7 (2016) 22016–22030.
- [23] Y. Peng, et al., USP39 Serves as a Deubiquitinase to Stabilize STAT1 and Sustains Type I IFN-Induced Antiviral Immunity, *J. Immunol.* 205 (2020) 3167–3178.
- [24] X. Li, et al., Deubiquitinase USP39 and E3 ligase TRIM26 balance the level of ZEB1 ubiquitination and thereby determine the progression of hepatocellular carcinoma, *Cell Death Differ.* 28 (2021) 2315–2332.
- [25] Z. Lin, et al., Ubiquitin-specific protease 22 is a deubiquitinase of CCNB1, *Cell Discov.* 1 (2015) 15028.
- [26] F.C. Nucifora Jr., et al., Ubiquitination via K27 and K29 chains signals aggregation and neuronal protection of LRRK2 by WSB1, *Nat. Commun.* 7 (2016) 11792.
- [27] M. Karim, et al., Nonproteolytic K29-Linked Ubiquitination of the PB2 Replication Protein of Influenza A Viruses by Proviral Cullin 4-Based E3 Ligases, *mBio* 11 (2020) e00305–e00320.
- [28] P. Gao, et al., E3 ligase Nedd41 promotes antiviral innate immunity by catalyzing K29-linked cysteine ubiquitination of TRAF3, *Nat. Commun.* 12 (2021) 1194.
- [29] C. Fei, et al., Smurf1-mediated Lys29-linked nonproteolytic polyubiquitination of axin negatively regulates Wnt/beta-catenin signaling, *Mol. Cell. Biol.* 33 (2013) 4095–4105.
- [30] P. Chastagner, A. Israel, C. Brou, Itch/AIP4 mediates Deltex degradation through the formation of K29-linked polyubiquitin chains, *EMBO Rep.* 7 (2006) 1147–1153.
- [31] H. Chen, et al., Overexpression of CDC2/CyclinB1 in gliomas, and CDC2 depletion inhibits proliferation of human glioma cells in vitro and in vivo, *BMC Cancer* 8 (2008) 29.